Wideband Quasi-Yagi Antenna with Broad-Beam Dual-Polarized Radiation for Indoor Access Points

Son Xuat Ta [1], Cong Danh Bui [3], and Truong Khang Nguyen [2,3,*]

[1] School of Electronics and Telecommunications
Hanoi University of Science and Technology, Ha Noi, Viet Nam
xuat.tason@hust.edu.vn

[2] Division of Computational Physics, Institute for Computational Science
Ton Duc Thang University, Ho Chi Minh City, Vietnam

[3] Faculty of Electrical and Electronics Engineering
Ton Duc Thang University, Ho Chi Minh City, Vietnam
*nguyentruongkhang@tdtu.edu.vn

Abstract ─ This paper presents a wideband, broad beamwidth, dual-polarized antenna for the indoor access points. Its primary radiating elements are two quasi-Yagi antennas, which are arranged orthogonally. The antenna element employs two balanced directors to broaden bandwidth and avoid the structural conflict of the orthogonal installation. A microstrip-slotline transformer is used in the feeding structure for allowing the wideband operation and high port-to-port isolation. The dual-polarized quasi-Yagi antenna is incorporated with a metallic cavity in order to improve the unidirectional radiation in terms of gain, front-to-back ratio, and beamwidth. The final prototype has been fabricated and tested. The antenna yielded a wide impedance bandwidth covering a frequency range from 1.64 to 3.0 GHz (60%) for both ports with port-to-port isolation of a higher than 25 dB. In addition, at both ports, the antenna achieves stable unidirectional radiation with broad beamwidth, high front-to-back ratio, and high radiation efficiency.

Index Terms ─ Balanced directors, beamdwidth, cavity-backed reflector, dual polarization, microstrip-slotline transformer, quasi-Yagi antenna.

I. INTRODUCTION

Quasi-Yagi antenna, which was first presented by Qian et al. in 1998 [1], has been one of the most popular choices for the modern wireless communication systems owing to its features of planar structure, broadband, high directivity, high front-to-back (F-B) ratio, low cross-polarization level, high efficiency, ease of realization and low cost. The basic configuration of a quasi-Yagi antenna includes a truncated ground plane acted as a reflector, a driver, and directors [2]. In order to be easily integrated with the other circuit components (e.g., printed power dividers, phase shifters …) or the standard connector, the quasi-Yagi antennas are normally fed by an unbalanced feed-line such as microstrip line [1–3] or coplanar waveguide [4–6]. Consequently, these antennas require a transformer between the driver and the feed-line. In the past years, the main considerations in designing the quasi-Yagi antenna are broadening bandwidth, reducing the size, and improving radiation characteristics. Several double dipole quasi-Yagi antennas [7–9] have been proposed for broadening the impedance matching bandwidth and achieving a small gain variation. The double-dipoles, however, increase the antenna size considerably. In [10], [11], the compact quasi-Yagi antennas with microstrip line to slotline transition achieved bandwidth > 90%. Recently, the bandwidth of a quasi-Yagi antenna was enlarged up to 94% by using metamaterial resonators [12]. However, due to the small reflector element, the antennas [10] – [12] yielded a relatively large back radiation. Also, their beamwidths are significantly different for the E- and H-plane radiation patterns.

On the other word, in order to achieve steady services regardless of place, a large number of indoor access points for the modern wireless communication systems are needed to be installed in shaded areas, such as tunnels, inside of high buildings, subway stations, as well as other underground areas. Antennas for the indoor access points [13–18] focus not only bandwidth but also radiation characteristics. The antennas with wideband characteristic [13], [16], were proposed for use in several wireless communication systems, while the multi-band antennas [14], [15] were designed for the systems operating in different frequency bands. To achieve the desired coverage, the antennas were developed to yield appropriate radiation characteristics such as high-gain

Submitted On: August 7, 2018
Accepted On: March 3, 2019

[14], wide beamwidth [15], or omnidirectional pattern [16]. The above access point antennas are linear polarization. Recently, dual-polarized antennas [17], [18] have been presented for the indoor access points to enhance the channel capacity and mitigate the effects of multipath fading. In [17], a dual-polarized antenna with an overall size of 70 mm × 70 mm × 14 mm achieved an operational bandwidth of about 16.4% (2.4 – 2.83 GHz), isolation of > 40 dB and the peak gain of 9 dBi. This antenna, however, requires a complicated feeding network, which includes microstrip-lines, metal shorting plates, and U-shaped microstrip coupling lines. In [18], a crossed enlarged dipole antenna using parasitic elements achieved an impedance bandwidth of about 44.5%, isolation of > 31 dB and gain of > 7.0 dBi. Its radiation patterns are not very symmetric, in particular, at the high frequencies. This could be attributed to the feeding structure; i.e., the crossed dipole elements are fed coaxial-lines directly.

In this paper, a wideband dual-polarized antenna with broad-beam radiation is presented. The antenna consists of two printed quasi-Yagi antenna elements, which are orthogonal and vertically placed at the center of a cylinder metallic cavity for achieving the broad-beam radiation and mitigating the difference for beamwidths of the E- and H-plane patterns. In order to avoid the structural conflict of the orthogonal installation, the quasi-Yagi antennas employ two directors, which are arranged symmetrically. The antenna elements are fed by a microstrip-slotline transformer for allowing the wideband operation and high port-to-port isolation. The proposed design was characterized via the ANSYS High-Frequency Structure Simulator (HFSS). The optimized prototype was fabricated and measured.

II. ANTENNA DESIGN AND CHARACTERISTICS

A. Antenna geometry

The geometry of the proposed antenna is illustrated in Fig. 1. It is composed of two printed quasi-Yagi antennas, which are orthogonal and vertically placed at the center of the metallic cavity. Each antenna element consists of a feeding structure of microstrip-slotline transformer, a driver, two directors, and a truncated ground plane. The microstrip-slotline transformer is composed of a folded microstrip-line and a rectangular slot. The quasi-Yagi antennas are printed on both sides of FR4 substrates with a dielectric constant of 4.4, a loss tangent of 0.02, and a thickness of 0.8 mm. For allowing the orthogonal installation without the structure conflict, the directors are arranged symmetrically and two slots are separately embedded in the antenna elements. The cavity has a cylindrical shape with 100-mm diameter and height of H_{cav}. The center frequency was chosen as 2.2 GHz. All of the antenna-designs were numerically simulated using the HFSS (ANSYS Electronics Desktop) version 17.1.

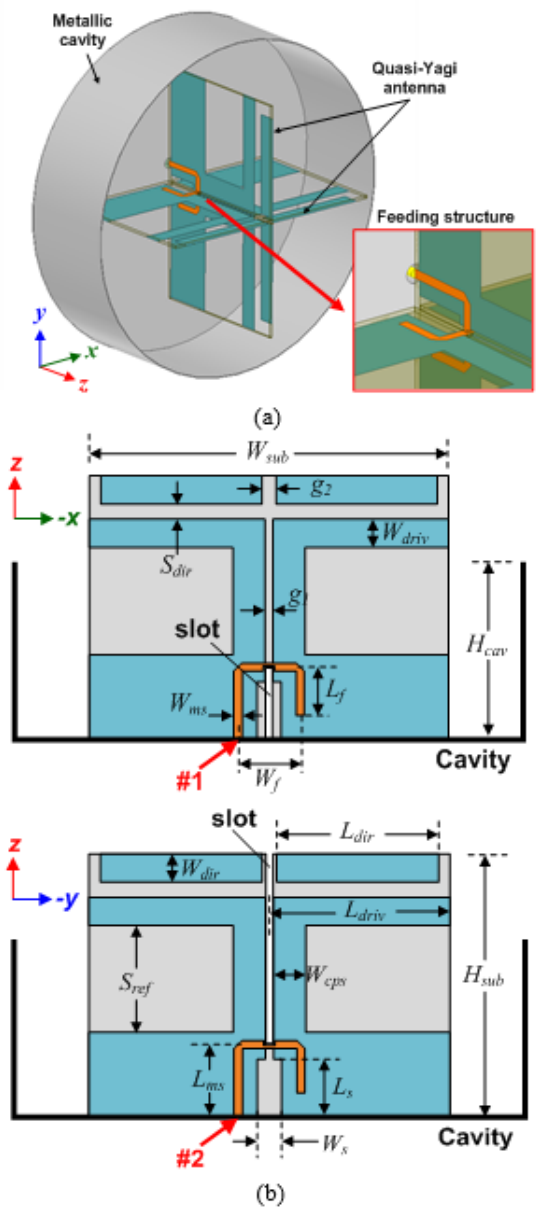

Fig. 1. Geometry of the proposed antenna: (a) perspective view and (b) cross-sectional views.

The solution type is set to a driven model. As the HFSS requirement, the radiation box walls are a quarter-wavelength (for the lowest frequency considered) away from the antenna for the desired accuracy in the calculation of the far-fields. The antenna is excited by two circular lumped ports that are renormalized to 50-Ω full port impedance at all frequencies. Two 10-mm coaxial

lines (d = 1.4 mm, D = 3.2 mm, ε_r = 1) were inserted between the lumped ports and the microstrip-lines. Real copper was used in all of the simulations, the conductivity being set to σ = 5.8 × 107 S/m, the relative permittivity being set to μ = 1, and without surface roughness. The dual-polarized antenna was optimized vias a series of the HFSS simulations to achieve a wideband operation, a high port-to-port isolation, a broad-beam radiation pattern, and a high front-to-back ratio. Its optimized design parameters are as follows: W_{sub} = 70, H_{sub} = 45, L_{gnd} = 15, S_{ref} = 17, W_{cps} = 6, L_{driv} = 35, W_{driv} = 5, S_{dir} = 3, L_{dir} = 30, W_{dir} = 5, W_s = 4, L_s = 10, W_f = 10, L_{ms} = 12, W_{ms} = 1.5, L_f = 8, g_1 = 1, g_2 = 2 and H_{cav} = 30 (Units: mm).

B. Evolution of the cavity-backed quasi-Yagi antenna element

Figure 2 shows the design evolution of the quasi-Yagi antenna, which was used as the primary radiation elements in the dual-polarized configuration. Ant. #1 is a planar quasi-Yagi antenna without a director and with a 100-mm truncated ground plane. Ant. #2 is Ant. #1 with adding two balanced directors. Ant. #3 is a quasi-Yagi antenna backed by a 100-mm diameter cavity reflector. Ants. #2 and #3 were optimized for a wideband characteristic at the 2.2 GHz center frequency. The design parameters of Ant. #3 are same as those of the proposed antenna, whereas the design parameters of Ant. #1 are same as those of the Ant. #2. Due to the planar configuration, the design parameters of Ant. #2 are slightly different from those of Ant. #3. Referring to Fig. 1 (b), the optimized parameters of Ant. #2 are as follows: W_{sub} = 100, H_{sub} = 50, L_{gnd} = 15, S_{ref} = 20, W_{cps} = 6, L_{driv} = 66, W_{driv} = 5, S_{dir} = 3, L_{dir} = 30, W_{dir} = 5, W_s = 4, L_s = 10, W_f = 10, L_{ms} = 12, L_f = 8, g_1 = 1, and g_2 = 2 (units: mm). The three configurations were characterized via the HFSS and their performances are given in Fig. 3.

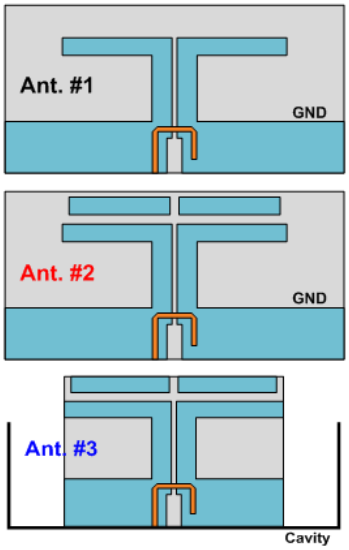

Fig. 2. Different configurations of quasi-Yagi antenna.

From Fig. 3 (a), the quasi-Yagi antenna without a director (Ant. #1) yielded two resonances of 1.7 GHz and 2.4 GHz in the examined frequency range. The presence of the directors broadened the bandwidth of the antennas; both configurations of Ant. #2 and Ant. #3 yielded three resonances and a significantly broader bandwidth as compared to Ant. #1. Also, the presence of directors improved the end-fire radiation of the planar quasi-Yagi antenna considerably. As shown in Figs. 3 (b, c), Ant. #2 had a higher gain and a higher F-B ratio over Ant. #1. Due to the natural radiation of the printed quasi-Yagi antenna, the beamwidth is significantly different for the E- and H-plane patterns. This difference was mitigated by using the cavity-backed reflector; i.e., the beamwidth of E-plane pattern was broadened, whereas the beamwidth of H-plane was narrowed. Also, the presence of the cavity produced an average increase of 2.1 dB in the gain relative to the planar antennas, as shown in Fig. 3 (b).

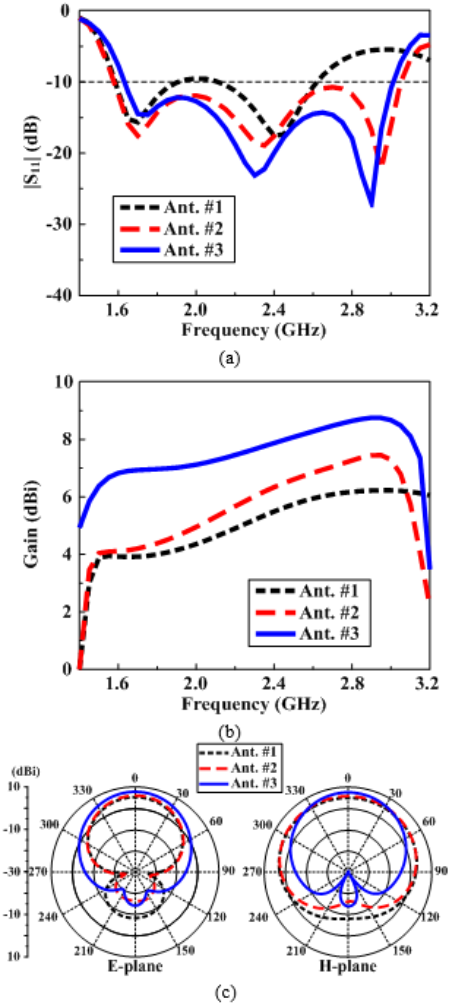

Fig. 3. Simulated (a) $|S_{11}|$, (b) gain, and (c) 2.2 GHz total-gain radiation patterns of the quasi-Yagi antenna in different configurations.

C. Cavity-backed reflector

As mentioned above, the radiation characteristics of the quasi-Yagi antenna were significantly improved by using the cavity reflector. For a better understanding of this issue, the performances of Ant. #3 were calculated for different heights of the cavity (H_{cav}) and given in Figs. 4 and 5. As H_{cav} increased, the resonances shifted toward the lower frequency [Fig. 4 (a)], whereas the radiation characteristics changed significantly; i.e., as shown in Fig. 4 (b), the gain decreased in the low-frequency region but increased in the high-frequency region. As shown in Fig. 4 (c), the F-B ratio improved with H_{cav} increasing from 0 mm to 30 mm, but degraded in almost the frequency range with the cavity height at 30-45 mm.

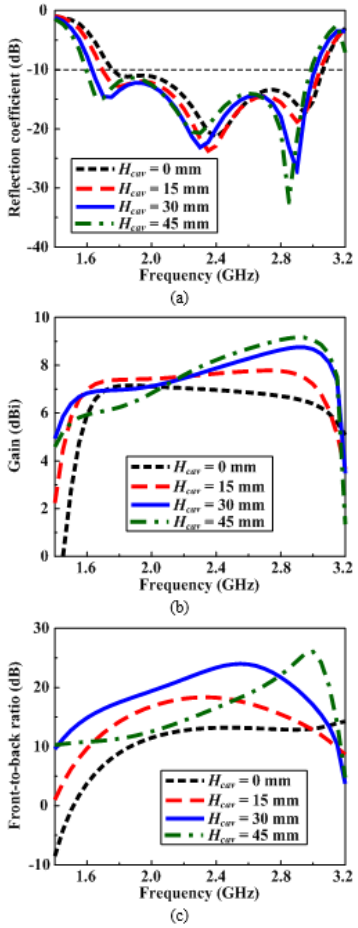

Fig. 4. Simulated (a) $|S_{11}|$, (b) gain, and (c) F-B ratio of Ant. #3 for different H_{cav}.

From Fig. 5, it is observed that with increasing H_{cav}, the beamwidth of E-plane pattern broadened, whereas the beamwidth of H-plane narrowed. With the cavity height of H_{cav} = 15 mm, the antenna offered the flattest gain (7.4 ± 0.4 dBi), an F-B ratio of > 10 dB at 1.6-3.0 GHz, and beamwidths of 71° and 91° for the E- and H-planes at 2.2 GHz, respectively. The antenna with H_{cav} = 30 mm yielded a gain of 7.7 ± 0.8 dBi, the highest F-B ratio at 1.6-3.0 GHz, and beamwidths of 76° and 80° for the E- and H-planes at 2.2 GHz, respectively. Therefore, H_{cav} = 30 mm was chosen for the final design based on a trade-off between the constant gain, the high front-to-back ratio and similar beamwidth in the *E*- and *H*-planes.

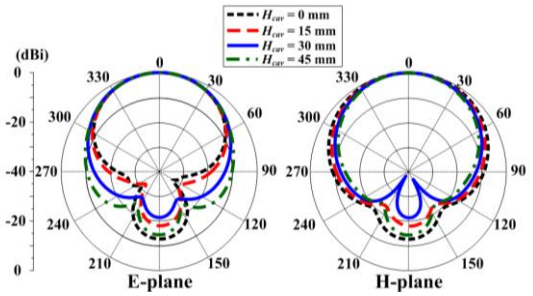

Fig. 5. Normalized 2.2 GHz total-gain radiation patterns of Ant. #3 for different H_{cav}.

III. FABRICATION AND MEASUREMENT

The dual-polarized quasi-Yagi antenna was realized and tested. A fabricated sample of the antenna is illustrated in Fig. 6. The quasi-Yagi antennas were fabricated by using printed circuit board technology, whereas the cavity was made of 0.2-mm copper sheets. The two orthogonal quasi-Yagi elements were vertically welded at the center of the cavity. Two coaxial-lines were used to feed the prototype; their inner parts passed through the cavity and connected to the microstrip-line of the transformer, whereas their outer parts were connected to the reflector. The prototype has a total volume of $\pi \times 50^2 \times 45$ mm^3.

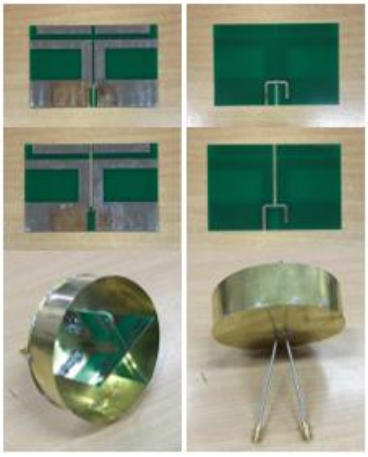

Fig. 6. Fabricated sample.

Figure 7 (a) illustrates the reflection coefficients of the fabricated antenna at two ports. The measurements

agreed rather closely with the simulations and both indicated a wideband operation. At Port #1, the measurement resulted in a reflection coefficient < -10 dB bandwidth of 1.59-2.97 GHz (60.5%), while the simulated bandwidth was 1.63-2.97 GHz (58.3%). At Port #2, the measured reflection coefficient < -10 dB was from 1.59 GHz to 3.06 GHz (63.2%), whereas the simulated value ranged from 1.64 GHz to 3.02 GHz (59.2%). The port-to-port isolation of the antenna is illustrated in Fig. 6 (b). The measurement resulted in isolation of > 25 dB relative to the simulated value of > 23 dB across the entire operating bandwidth. There was a slight difference between the measured and HFSS predicted results. This difference could be attributed the fabrication tolerances and the effects of tin-conductor (not included in the simulations), which was used to coat the copper part of the printed quasi-Yagi antennas and to weld the coaxial lines and the feeding structure.

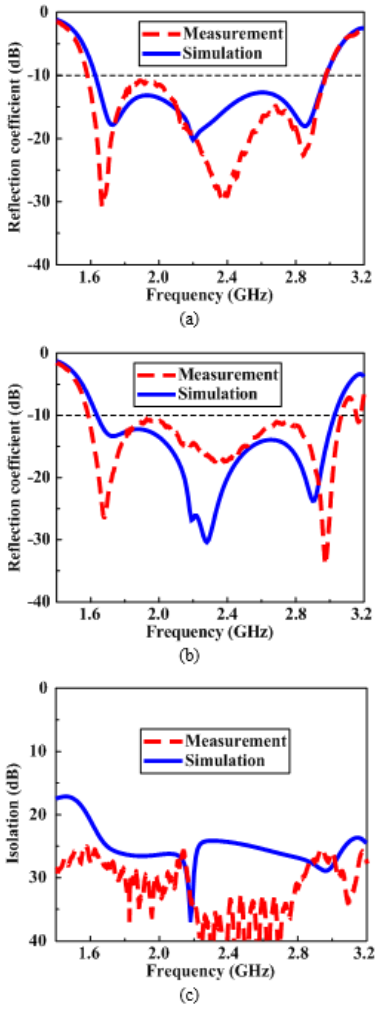

Fig. 7. Simulations and measurements of the dual-polarized quasi-Yagi antenna: reflection coefficients at: (a) Port #1, (b) Port #2, and (c) port-to-port isolation.

Figure 8 shows the radiation patterns of the prototype for Port #1 excitation. Again, there is a good agreement between measurement and simulation. It is observed that the antenna yielded good unidirectional radiation with a highly symmetric profile, high F-B ratio, and wide beamwidth. The F-B ratio is > 20 dB at all examined frequencies. As the frequency increased from 1.6 GHz to 3.0 GHz, half-power beam width (HPBW) in the E-plane is decreased from about 94° to 60°, whereas the HPBW in the H-plane is decreased from about 100° to 70°. Due to the structure symmetry, the results of the prototype for Port #2 are almost identical to those of Port #1, thus, they are not shown for brevity.

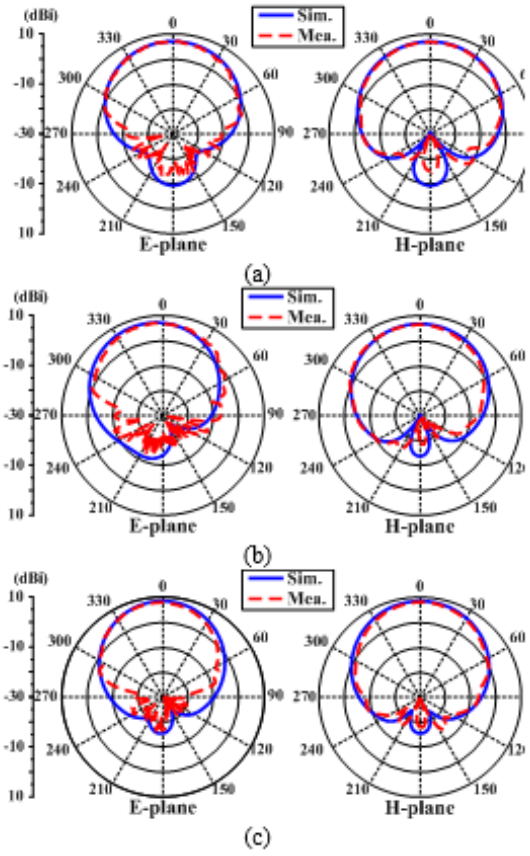

Fig. 8. Measured and simulated total-gain radiation patterns of the dual-polarized quasi-Yagi antenna at port #1: (a) 1.7 GHz, (b) 2.2 GHz, and (c) 2.7 GHz.

Figure 9 shows the measured and simulated gains of the antenna prototype. Within the operational bandwidth, the antenna yielded measured broadside gains of 6.4-7.0 dBi and 6.0-8.0 dBi for the ports #1 and #2, respectively, as compared to the simulated values of 6.9-8.5 dBi for both ports. In addition, the measurement resulted in radiation efficiency better than 75% as compared to the simulated value of > 80% when exciting from either port. The measured gain and radiation efficiency were slightly

smaller than the HFSS simulated values. This difference could be attributed to a difference in the dielectric loss used in our simulation and the real value in the measurement.

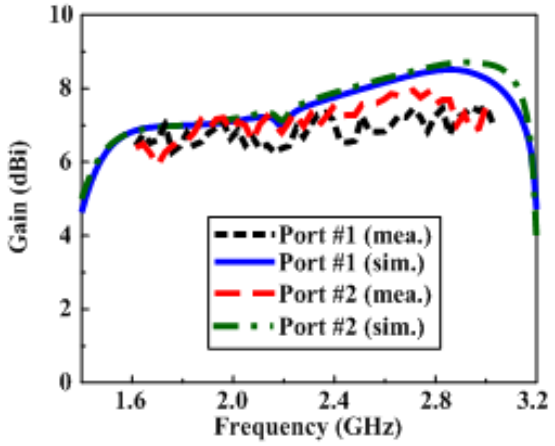

Fig. 9. Simulation and measurement gain of the dual-polarized quasi-Yagi antenna.

In order to signify how the two elements of the proposed antenna are coupled to each other, the envelope correlation coefficient (ECC) was calculated from the S-parameters using the following formula [19]:

$$\mathrm{ECC} = \frac{|S_{11}^{*}S_{12} + S_{21}^{*}S_{22}|}{(1-|S_{11}|^2-|S_{12}|^2)(1-|S_{21}|^2-|S_{22}|^2)}. \quad (1)$$

The simulated and measured ECC values of the fabricated antenna are shown in Fig. 10. Both simulation and measurement indicated that the ECC was less than 0.001 within its impedance matching bandwidth. As a result, the two elements of the proposed antenna have a very small coupling to each other.

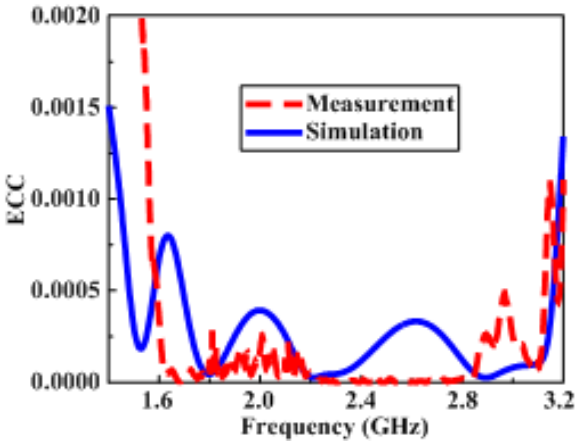

Fig. 10. simulated and measured ECCs of the dual-polarized quasi-Yagi antenna.

IV. CONCLUSION

A cavity-backed quasi-Yagi antenna with wideband and broad-beam dual-polarized radiation has been presented for use in the indoor access points. The antenna consists of two orthogonal printed quasi-Yagi antennas, which are fed by a microstrip-slotline transformer to allow the wideband operation and high port-to-port isolation. The quasi-Yagi antenna elements employed two balanced directors to not only broaden the frequency bandwidth but also avoid the structural conflict of the orthogonal installation. The cavity-backed reflector is utilized for improving the unidirectional radiation of the antenna element in terms of gain, front-to-back ratio, and beamwidth. The final prototype resulted in an impedance matching bandwidth of > 60% for both ports and isolation of > 25 dB. Its operational bandwidth completely covers DCS/PCS/UMTS/LTE 1, 2, 3, 4, 7, 9, 10, 15, 16, 23, 25/WiMAX 2.3 GHz, 2.5 GHz/WLAN 2.4-GHz bands (1710 – 2690 MHz). Moreover, at both ports, the antenna achieves stable unidirectional radiation with broad beamwidth, high front-to-back ratio, and high radiation efficiency.

ACKNOWLEDGMENT

This research is funded by Vietnam National Foundation for Science and Technology Development (NAFOSTED) under grant number 102.04-2016.02.

REFERENCES

[1] Y. Qian, W. R. Deal, N. Kaneda, and T. Itoh, "Microstrip-fed quasi-Yagi antenna with broad-band characteristics," *Electron. Lett.*, vol. 34, no. 23, pp. 2194-2196, Nov. 1998.

[2] N. Haneda, W. R. Deal, Y. Qian, R. Waterhouse, and T. Itoh, "A broad–band planar quasi–Yagi antenna," *IEEE Trans. Antenna Propagat*., vol. 50, no. 8, pp. 1158-1160, Aug. 2002.

[3] S. X. Ta, B. Kim, H. Choo, and I. Park, "Wideband quasi-Yagi antenna fed by microstrip-to-slotline transition," *Microwave Opt. Technol. Lett*., vol. 54, no. 1, pp. 150-153, July 2012.

[4] J. Sor, Y. Qian, and T. Itoh, "Coplanar waveguide fed quasi–Yagi antenna," *Electronics Letters*, vol. 36, no. 1, pp. 1-2, Jan. 2000.

[5] H. K. Kan, R. B. Waterhouse, A. M. Abbosh, and M. E. Bialkowski, "Simple broadband planar CPW-fed quasi-Yagi antenna," *IEEE Antenna Wireless Propagate. Lett*., vol. 6, pp. 18-20, 2007.

[6] Z. Du, Z. Wu, M. Wang, J. Rao, and P. Lue, "Compact quasi-Yagi antenna for handheld UHF RFID reader," *ACES Journal*, vol. 30, no. 8, pp. 860-865, Aug. 2015.

[7] A. A. Eldek, "Ultrawideband double rhombus antenna with stable radiation patterns for phased array applications," *IEEE Trans. Antenna Propag*., vol. 55, no. 1, pp. 84-91, Jan. 2007.

[8] S. X. Ta, H. Choo, and I. Park, "Wideband double-dipole Yagi-Uda antenna fed by a microstrip-slot coplanar stripline transition," *Progress in Electromagnetics Research B*, vol. 44, pp. 71-87, 2012.

[9] J. Wu, Z. Zhao, Z. Nie, and Q. Liu, "Bandwidth enhancement of a planar printed quasi-Yagi antenna with size reduction," *IEEE Trans. Antenna Propagat*., vol. 62, no. 1, pp. 463-467, Jan. 2014.

[10] J. Wu, Z. Zhao, Z. Nie, and Q. Liu, "Design of a wideband planar printed quasi-Yagi antenna using stepped connection structure," *IEEE Trans. Antenna Propagat*., vol. 62, no. 6, pp. 3431-3435, June 2014.

[11] J. Yeo and J. Lee, "Bandwidth enhancement of double dipole quasi-Yagi antenna using stepped slotline structure," *IEEE Antennas Wireless Propag. Lett*., vol. 15, pp. 694-697, 2016.

[12] M. Aeini, S. Jarchi, and S. Faraji-Dana, "Compact, wideband-printed quasi-Yagi antenna using spiral metamaterial resonators," *Electron. Lett.*, vol. 53, no. 21, pp. 1393-1394, Oct. 2017.

[13] C. R. Medeiros, E. B. Lima, J. R. Costa, and C. A. Fernandes, "Wideband slot antenna for WLAN access points," *IEEE Antennas Wireless Propag. Lett.*, vol. 9, pp. 79-82, 2010.

[14] S. W. Su, "High-gain dual-loop antennas for MIMO access points in the 2.4/5.2/5.8 GHz bands," *IEEE Trans. Antennas Propag.*, vol. 58, no. 7, pp. 2412-2419, July 2010.

[15] S. X. Ta, J. Han, H. Choo, and I. Park, "Dual-band printed dipole antenna with wide beamwidth for WLAN access points," *Microw. Opt. Technol. Lett.*, vol. 54, no. 12, pp. 2806-2811, Dec. 2012.

[16] Z. Y. Zhang, G. Fu, W. J. Wu, J. Lei, and S. X. Gong, "A wideband dual-sleeve monopole antenna for indoor base station application," *IEEE Antennas Wireless Propag. Lett.*, vol. 10, pp. 45-48, 2011.

[17] J. Lee, K. Lee, and P. Song, "The design of dual-polarized small base station antenna with high isolation having a metallic cube," *IEEE Trans. Antennas Propag*., vol. 63, no. 2, pp. 791-795, Feb. 2015.

[18] H. Lee and B. Lee, "Compact broadband dual-polarized antenna for indoor MIMO wireless communication systems," *IEEE Trans. Antennas Propag*., vol. 64, no. 2, pp. 766-770, Feb. 2016.

[19] L. Chen, J. Hong, and M. Amin, "A compact CPW-fed MIMO antenna with band-notched characteristic for UWB system," *ACES Journal*, vol. 33, no. 7, pp. 818-821, July 2018.